Modification of Nanocellulose with a Xyloglucan–RGD Conjugate Enhances Adhesion and Proliferation of Endothelial Cells: Implications for Tissue Engineering

Aase Bodin,[†] Lage Ahrenstedt,[‡] Helen Fink,[§] Harry Brumer,[‡,⊥] Bo Risberg,[§] and Paul Gatenholm*[,†]

Biopolymer Technology, Department of Chemical and Biological Engineering, Chalmers University of Technology, SE-412 96 Gothenburg, Sweden, School of Biotechnology, Royal Institute of Technology, Alba Nova University Centre, SE-106-91 Stockholm, Sweden, and Vascular Engineering Centre, Institution of Clinical Sciences, Department of Surgery, Sahlgrenska University Hospital, Gothenburg, Sweden

Received March 27, 2007; Revised Manuscript Received September 24, 2007

This paper describes a novel method for introducing the RGD cell adhesion peptide to enhance cell adhesion onto bacterial cellulose (BC). BC and cotton linters as reference were modified with xyloglucan (XG) and xyloglugan bearing a GRGDS pentapeptide. The adsorptions followed Langmuir adsorption behavior, where both XGs probably decorate the cellulose surfaces as a monolayer. The adsorption maximum of the XGs reached around 180 mg/g on BC and only about three times as much on cotton linters. The adsorption was verified with colorimetric methods. The specific surface area of BC measured with XG and XG-GRGDS was about 200 m^2/g and was almost three times less for cotton linters, 60 m^2/g. The difference in the amounts of XGs adsorbed might be explained by the swollen network of bacterial cellulose and a more exposed and accessible bulk as compared to cotton linters. The nanocellulose material was modified homogeneously throughout the material, as seen by the z-scan in confocal microscopy. Moreover, the modification in the water phase, in comparison with organic solvents, was clearly advantageous for preserving the morphology, as observed with SEM. The modification slightly increased the wettability, which might explain the decrease in or undetectable adsorption of adhesive protein shown by QCM-D. Initial cell studies showed that adhesion of human endothelial cells is enhanced when the BC hydrogel is modified with XG-GRGDS. QCM-D studies further revealed that the cell enhancement is due to the presence of the RGD epitope on XG and not to a nonspecific adsorption of fibronectin from cell culture medium. Optimization and proliferation studies of human endothelial cells onto bacterial cellulose modified with XG-GRGDS are currently being carried out at the Vascular Engineering Center, Sahlgrenska University Hospital, Gothenburg.

Introduction

Several polymers are currently used in applications in which they are in contact with blood, for example, catheters, blood bags, blood vessel replacements, membranes for dialysis, cardiac valves, and so on. Despite improvements of the polymers available and extensively used in contact with blood, they are still very unsatisfactory. There are as yet problems with protein adsorption to these materials and compliance mismatch with the natural blood vessel wall when used as a blood vessel replacement.[1] Both events lead to platelet activation, aggregation, and, in severe cases, blood clots. Synthetic materials can be used for larger vessels, but their low hemocompatibility renders them useless in coronary applications or below-the-knee arterial replacements. Extensive research and trials have been conducted to seed endothelial cells onto expanded polytetrafluoroethylene (ePTFE) tubes and to make surface modifications with heparin.[2–5] However, problems have been encountered in keeping the cells or the heparin on the surface in the long term.[6,7]

Cellulose derivatives such as ethyl, methyl, amino ethyl, and acetate phtalate are among the polymers that have been extensively used in applications such as blood purifier, anticoagulant, and plasma expander in aqueous systems.[8,9] Cellulose, especially hydroxypropyl cellulose, is an attractive polymer as a matrix in applications such as drug delivery for sustained release dosage.[10] Similar to synthetic polymers, cellulose originating from plants has been modified to achieve satisfying hemocompatibility.[11,12] Another source of cellulose that has completely different properties than those of plant cellulose is bacterial cellulose (BC). BC has been shown to be interesting as a biomaterial, mainly because of its high purity and biocompatibility and the possibility to mold it into different shapes for a given application.[13–15] BC is an exopolysaccharide and is produced fairly inexpensively by cultivating *A. xylinum.* Compared with plant cellulose, the BC is extruded in its pure form and is not associated with any other polymers or proteins. BC can be effectively purified with sodium hydroxide, achieving endotoxin values compliant with FDA requirements for implants in contact with blood, that is, <20 EU per device.[16] BC contains 99% water and can be seen as a hydrogel, albeit not by definition as it is not a network of polymer chains that are water soluble. Despite its low solid content, the ramified network of nanocellulose fibrils provides good mechanical properties.

The great interest in hydrogels for a variety of biomedical and pharmaceutical applications is based on their commonly structural resemblance to the extracellular matrix (ECM) of many tissues, for example, collagen and proteoglycans. With

* To whom correspondence should be addressed. E-mail: Paul.Gatenholm@chalmers.se.
[†] Chalmers University of Technology.
[‡] Royal Institute of Technology.
[§] Sahlgrenska University Hospital.
[⊥] Fellow of the Swedish Research Council.

10.1021/bm070343q CCC: $37.00
Published on Web 11/22/2007

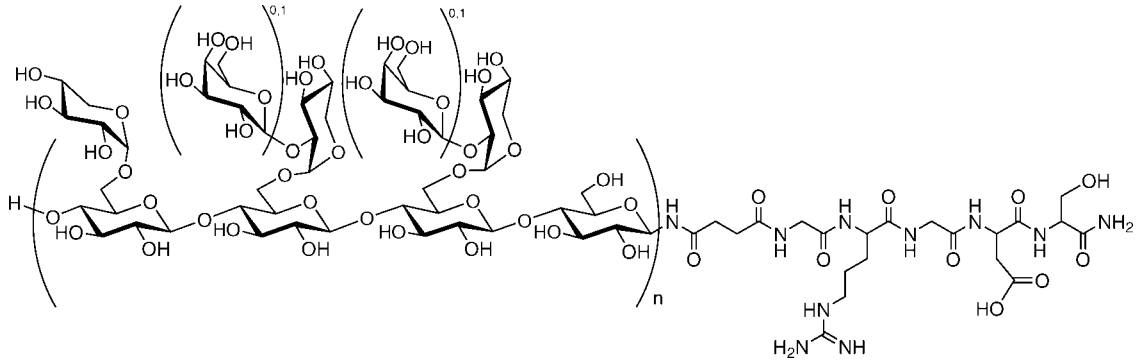

Figure 1. Structure of the XGO-succ-GRGDS ($n = 1$) and XG-GRGDS ($n \approx 30$, M_w 32000, M_w/M_n 1.7) glycoconjugates produced by solid phase synthesis and XET catalysis. Variable galactosylation of the oligo- and polysaccharide is indicated. At physiological pH (7.4), the R groups of arginine and aspartic acid will be positively and negatively charged, respectively.

the exception of collagen, cells do not have receptors to hydrogel forming polymers and thus cannot adhere. Furthermore, because of the hydrophilic nature of the hydrogels, ECM proteins containing cell surface receptors, such as laminin, fibronectin, and vitronectin, typically do not readily adsorb to the gel surface. This property makes the hydrogel polymer highly biocompatible because it hinders such cells as platelets from adhering.[17]

Because the interactions that lead to surface-induced thrombosis occur at the blood–biomaterial interface, surface modification is a way to increase hemo-compatibility.[18] Among the different modifications, modifications with polysaccharides such as heparin have also been widely used to minimize thrombus formation on artificial organs. A problem, however, has been that the activity of heparin significantly decreases when it is directly bound to a surface. To date, the most successful type of biocompatible surface has been the end-point-attached heparin surface.[19,20] Another attractive surface modification has been to introduce hydrophilic groups that can prevent plasma protein adsorption, platelet adhesion, and thrombus formation. The problem has been to get them to remain on the surface for long-term devices such as vascular grafts. Especially, water soluble polymers, such as polyacrylamide (PAAm), poly(*N*,*N*-dimethylacrylamide) (PDMAAm), poly(ethylene glycol) (PEG), ethylene–vinyl alcohol copolymer (EVA), and poly (2-hydroxyethyl methacrylate) (PHEMA), have been grafted onto solid surfaces to prevent protein adsorption.[21–24] Other ideas for modifying a material to improve its hemocompatibility have to do with mimicking the biologically inert surface.[25] In a blood vessel, this inert surface is composed of a monolayer of endothelial cells. Current materials used as vascular grafts, such as ePTFE and polyester, do not promote adhesion or proliferation of human endothelial cells. Surface modification has therefore been done with either fibrinogen, fibronectin, or immobilized RGD (Arg-Gly Asp), which is the minimal fragment of the active site of adhesive proteins such as fibrinogen, fibronectin, and the von Willbrand factor.[26–28]

The aim of this study was to surface modify BC with xyloglucan–GRGDS (XG-GRGDS) conjugates (Figure 1). Using aqueous chemo-enzymatic techniques for the surface modification of cellulose, in combination with exploiting the well-known ability of endothelial cells to bind to peptides containing the RGD epitope, we introduce a specific peptide sequence to improve cell attachment and proliferation on BC.[29–31] We see potential applications of this new functional biomaterial as scaffolds for tissue engineering blood vessels.

Materials and Methods

Materials. BC hydrogel and Whatmann filter paper, grade 1, made from pure cotton linter used for comparison were investigated in adsorption studies of Congo Red and XG. Trimethylsilyl cellulose (TMSC) was used in the adsorption study using QCM-D. The TMSC was synthesized as described elsewhere and provided by courtesy of Professor Allan Esker.[32] BC was grown statically in a corn steep liquid medium, described elsewhere,[33] using Roux flasks (working volumes of 100 mL) at 30 °C for 3 days, giving a pellicle of 2 mm. The strain used for the biosynthesis was *Acetobacter xylinum* subsp. *sucrofermentas* BPR2001, trade number: 1700178. The strain was purchased from the American type Culture Collection. The BC was purified by boiling in 0.1 M NaOH, 60 °C, for 4 h and, thereafter, repeated boiling in Millipore water. The material was steam sterilized and stored refrigerated before use. BC was treated with acetone overnight prior to freeze-drying and SEM analysis.

Preparation of Xyloglucan and Xyloglucan–GRGDS. A mixture (15:7:32:46) of XXXG, XLXG, XXLG, and XLLG xyloglucooligosaccharides (XGOs) was obtained by direct treatment of tamarind (*Tamarindus indica*) kernel powder (60% XG content, D.N. Palani, Mumbai, India) by an *endo*-glucanase digestion, essentially as previously described.[34] The XGOs were activated by conversion to the corresponding 1-deoxy-1-aminosuccinamate derivatives (XGO-succ) via the 1-deoxy-1-amino-β-glycosides as follows. XGO (1 g, 0.78 mmol) was dissolved in deionized water (10 mL), followed by an addition of ammonium hydrogen carbonate (2.5 g). The mixture was then stirred at 42 °C for 28 h, with a continuous addition of ammonium hydrogen carbonate to maintain saturation.[35] The progress of the reaction was followed by TLC (70/30 acetonitrile/water). Excess ammonium hydrogen carbonate was removed by three cycles of freeze-drying to yield a white powder consisting of a mixture of XGOs and 1-deoxy-1-amino-β-glycosides; the extent of conversion was 83%, evaluated by integration of ^{1}H NMR signals from the anomeric protons of the starting material and product. The crude product was dissolved in water (10 mL), succinic anhydride (157 mg, 1.57 mmol, 2 equiv) was added, and the solution was vigorously stirred on a vortex mixer for 10 min.[36] Reversed-phase (C18 silica gel) chromatography using stepwise elution with water/acetonitrile mixtures containing 0.1% TFA yielded XGO-succinamate as a white powder (860 mg, 0.63 mmol, 80% yield over two steps). ^{1}H NMR (500 MHz, D_2O, 25 °C): δ 2.56 (t, $J = 6$ Hz, 2H, $COCH_2CH_2COOH$), 2.61 (t, $J = 7$ Hz, 2H, $COCH_2CH_2COOH$), 3.24–3.95 (m, H-2 to H-6 of Gal, Glc, 1-deoxy-1-aminosuccinate-Glc and H-2 to H-5 of Xyl), 4.44–4.50 (m, H-1 of Glc and Gal), 4.85–4.89 (m, H-1 of Xyl), 5.08–5.10 (m, H-1 of Xyl bearing Gal-β(1–2)). ESI-MS[37] XXXG-succ calcd $[M + 2Na]^{2+}$, 603.6802; found, 603.7095; XLXG-succ and XXLG-succ calcd $[M + 2Na]^{2+}$, 684.7066; found, 684.7079; XLLG-succ calcd $[M + 2Na]^{2+}$, 765.7330; found, 765.7473.

The GRGDS pentapeptide was synthesized on a 0.25-mmol scale using standard solid phase Fmoc chemistry according to the protocol described by Engfeldt et al.[38] with the following exceptions. The Fmoc-protected amino acids were activated with HBTU and HOBt (both 0.45 M in DMF) in the presence of DIPEA (2.0 M in NMP). Capping steps were excluded. Following the final Fmoc cleavage step, the peptide substitution of the resin was determined to be 0.47 mmol/g. XGO-succ was manually conjugated to the resin bound peptide in a reaction vessel equipped with a glass filter (pore size P2). XGO-succ (260 mg, 2 equiv) was dissolved in DMF (6 mL) and activated with HBTU (215 mg, 6 equiv) and HOBt (87 mg, 6 equiv) in the presence of DIPEA (66 mL, 4 equiv). The resin-bound peptide (200 mg, 1 equiv) was then added. The coupling was terminated after 1 h by the extensive washing of the resin with ethanol, NMP, DIPEA (5% in DCM), NMP, and DCM (10 mL each). The resin was subsequently dried under vacuum. The glycopeptide was cleaved from the resin with simulaneous removal of the side chain protection groups with 3 mL of TFA/H_2O/TIS (95:2.5:2:5) for 30 min at room temperature. The reaction was diluted with water (40 mL), extracted with tBME (3 × 40 mL), and filtered through glass fibers. Freeze-drying the aqueous phase yielded a white solid (82 mg, 47% yield). Under identical conditions, cleavage and deprotection of the unmodified peptide from 75 mg of resin yielded 15 mg of GRGDS (90% yield).

GRGDS: ^{1}H NMR (500 MHz, D_2O, 25 °C): δ 1.52–1.81 (m, 4H, 2 H$^{\beta}$-Arg, 2H$^{\chi}$-Arg), 2.65 (d, J = 6.5 Hz, 2H, H$^{\beta}$-Asp), 3.16 (t, J = 7 Hz, 2H, H$^{\delta}$-Arg), 3.80–3.92 (m, 6H, 4 H$^{\alpha}$-Gly, 2 H$^{\beta}$-Ser), 4.26 (t, J = 7 Hz, 1H, H$^{\alpha}$-Arg), 4.35 (t, J = 5 Hz, 1H, H$^{\alpha}$-Ser), 4.60 (t, J = 6.5 Hz, 1H, H$^{\alpha}$-Asp). ESI-MS calcd $[M + H]^+$, 490.2376; found, 490.2109.

XGO-succ-GRGDS: δ 1.53–1.86 (m, 4H, 2 H$^{\beta}$-Arg, 2H$^{\chi}$-Arg), 2.55–2.60 (m, 2H, H$^{\beta}$-Asp), 2.80–2.92 (m, 4H, XGO-NH-COCH_2CH_2CO-Gly), 3.12–3.16 (m, 2H, H$^{\delta}$-Arg), 3.25–3.98 (m, H$^{\alpha}$-Gly, H$^{\beta}$-Ser, H-2 to H-6 of Gal, Glc, 1-deoxy-1-aminosuccinate-Glc and H-2 to H-5 of Xyl), 4.25–4.30 (m, 1H, H$^{\alpha}$-Arg), 4.34–4.36 (m, 1H, H$^{\alpha}$-Ser), 4.68–4.74 (m, H-1 of Glc and Gal), 4.87–4.91 (m, H-1 of Xyl), 5.09–5.11 (m, H-1 of Xyl bearing Gal-β(1–2)). ESI-MS: XXXG-succ-GRGDS calcd $[M + H + Na]^{2+}$, 828.2988; found, 828.3080; XXLG-succ-GRGDS and XLXG-succ-GRGDS calcd $[M + H + 2Na]^{3+}$, 613.8800; found, 613.8911; calcd $[M + H + Na]^{2+}$, 909.3252; found, 909.3289; XLLG-succ-GRGDS calcd $[M + H + 2Na]^{3+}$, 667.8976; found, 667.9045; calcd $[M + 3Na]^{3+}$, 675.2249; found, 675.2198; calcd $[M + H + Na]^{2+}$, 990.3516; found, 990.3554.

The final XG-GRGDS glycoconjugate was prepared using XG *endo*-transglycosylase (XET)-mediated coupling[29] as follows. Tamarind XG (Megazyme, Ireland) was dissolved in water (2 mg/mL), and 200 mL was mixed with XGO-succ-GRGDS (100 mL, 2 mg/mL in H_2O), H_2O (50 mL), and a solution of the *Ptt*XET16A[39] enzyme (0.4 units/mL, 50 mL in 100 mM NaOAc, pH 5.5). The reaction was terminated after 35 min by heating the solution to 85 °C for 1 h. Denatured enzyme was removed by filtration on a glass fiber filter, and the product was precipitated from the filtrate by the addition of ethanol (3 vol). The precipitate was collected on a glass fiber filter and redissolved by stirring and gentle heating of the filter in water (20 mL). The resulting solution was freeze–dried to yield 390 mg of XG-GRGDS. Analysis by HP-SEC in DMSO, as described in ref 29, indicated that the product had a M_w value of 32000 (M_w/M_n 1.7). Unmodified XG with a similar molecular mass (M_w 36000, M_w/M_n 1.5) was produced using the same procedure, except that XGOs were substituted for XGO-succ-GRGDS.

Adsorption of Congo Red. The specific surface area of BC and cotton as a reference was evaluated by determining the maximum amount of adsorbed Congo Red dye (Direct Red 28, Purchased from Riedel-de Haën, Germany) following the procedures of Inglesby and Zeronian.[40,41] A total of six Whatman papers No. 1 and six BC gels were used at each adsorption concentration. The cellulose materials were exposed to Congo Red in 4 mL of aqueous solution containing 0.5, 1.5, 2.0, 2.5, 3.0, 3.5, 4.0, 4.5, and 5.0 (w/w) of Congo red and dyed for 24 h at 60 °C with a liquid ratio of 100:1. NaCl (20% w/w) was added as an electrolyte. The residual concentration [E, mg/mL] of Congo Red was calculated from the UV adsorption at 492 nm using a standard curve. The amount of Congo Red adsorbed on fiber [A, mg/g] was calculated from the difference in adsorption at 492 nm of the solution before and after the binding reaction, divided by the mass of fiber per volume of solution.

Adsorption of XG and XG-GRGDS. The specific surface areas of BC and cotton linters as a reference were evaluated by determining the maximum amount of XG and XG-GRGDS adsorbed. A total of six Whatman papers No. 1 and six BC gels were used at each adsorption concentration. The cellulose materials were immersed in 4 mL of aqueous solution containing 5, 10, 15, and 20% (w/w) of XG or XG-GRGDS. The XG adsorbed was measured by the colorimetric method described by Kooiman.[42] A total of 200 μL was withdrawn at various time intervals from 0 to 48 h and mixed with 1 mL of a 5:1 solution of 20% (w/v) Na_2SO_4 and triiodide solution (0.5% I_2 + 1% KI). The residual concentration [E, mg/mL] of XG was calculated from the adsorption at 620 nm using a standard curve. The amount of XG adsorbed on the fiber [A, mg/g] was calculated from the difference in adsorption at 620 nm of the solution before and after the binding reaction, divided by the mass of fiber per volume of solution.

Specific Surface Area. The specific surface area of cotton linters and BC derived from adsorption of Congo Red versus XG and XG-GRGDS was calculated using equation 1 derived from Langmuir's adsorption theory:[44]

$$\frac{[E]}{[A]} = \frac{1}{K_{ads}[A]_{max}} + \frac{[E]}{[A]_{max}} \quad (1)$$

where [E] (mg/mL) is the concentration of adsorbate at adsorption equilibrium, [A] (mg/g cellulose sample) is the amount of adsorbate adsorbed to the cellulose surface, [A_{max}] (mg/g cellulose sample) is the maximum amount of adsorbate adsorbed to the cellulose surface, and K_{ads} is the adsorption equilibrium constant. The specific surface, A_{sp}, is expressed as:

$$A_{sp} = \frac{[A]_{max} N_A A_{CR}}{10^{21} M_w} \quad (2)$$

where M_w is the molecular weight of Congo Red (653 g/mol), XG (36000 g/mol), and XG-GRGDS (32000 g/mol), N_A is Avogadro's constant, and A_{CR} is the area occupied by one Congo Red (1.73 nm^2), XG (69 nm^2), and XG-GRGDS (61 nm^2). Values for Congo Red were calculated by Ougiya et al.[43] Values for XG and XG-GRGDS were derived by presuming a linear decrease in the occupied area of an XG with molecular weight, that is, extrapolating from Ougiya et al. Values of A_{CR} ranged from 1870 nm^2 for high molecular weight XG (980 000 g/mol) to lower molecular weight XG, that is, 32000 and 36000 g/mol.

Scanning Electron Microscopy (SEM). SEM was used to study the surface morphology of the unmodified and modified cellulose materials. The BC materials were quenched in liquid nitrogen prior to freeze-drying. The surfaces were then coated with gold before analysis. This was done with a Zeiss DSM 940A operated at 10 kV.

Confocal Laser Microscope. Confocal microscopy equipped with a fiber coupled Ar Kr laser was used to study the morphology of BC in its wet state and the modification throughout the gel. Filters were chosen with regard to the emission wavelength of the dye [λ_{ex} = 495 nm and λ_{em} = 516]. The wet BC samples were fluorescently labeled by a fluorescently labeled XG (XG-FITC). XG-FITC was synthesized as described elsewhere and provided by courtesy of Dr. Qi Zhou, KTH Biotechnology.[29] The wet gel was stained for 24 h with a stock solution of 2 mg/mL XG-FITC. After staining, excess XG-FITC was removed by placing the samples in deionized water with mild stirring overnight.

Electron Spectroscopy for Chemical Analysis (ESCA). The chemical composition of BC was determined with ESCA before and after surface modification with XGs. The materials were oven-dried at 30 °C after modification and prior to the measurements. A Quantum 2000 from Physical Electronics was used for the measurements.[44] The area analyzed was 500 × 500 μm^2 and the beam size was 100 μm. The angle between the sample and the detector was 45 °C. The peak

intensities were measured and curve fitting was done using MultiPak software from Physical Electronics. Characteristic ESCA spectra of cellulose has one peak at 286.7 eV corresponding to carbon single-bonded to oxygen and one at 287.9 eV corresponding to carbon bonded to two oxygens. The relative amounts of different bound carbon were calculated with Gaussian curve fitting of the highest resolution C1s peak. The different positions of the C–C, C–O, O–C–O, and C═O or O–C═O were 285.0 ± 0.2 eV, 286.7 ± 0.2 eV, 281.1 ± 0.2 eV, and 289.4 ± 0.2 eV, respectively.

Dynamic Contact Angle toward Water. Static contact angle measurements were made on six oven-dried cellulose films, unmodified as well as modified with XG or XG-GRGDS. A 5 μL liquid droplet was applied to each cellulose surface. The contact angle, θ_e, was measured using a goniometer by registering the angle formed between the solid and the tangent to the drop surface.

Protein Adsorption using Quartz Crystal Microbalance with Dissipation Monitoring (QCM-D). A QCM-D instrument was used (Q-sense AB, Göteborg, Sweden) to study the adsorption of proteins to the cellulose surface as an effect of surface modification. The model cellulose surfaces were prepared on gold-plated QCM-D crystals. Surfaces were cleaned in an UV/ozone chamber for 10 min, followed by immersion in a 5:1:1 mixture of Milli-Q water, H_2O_2 (30%) and NH_3 (25%) for 10 min at 70 °C. The surfaces were washed with Milli-Q and dried with nitrogen. Trimethylsilyl cellulose (1 mg/mL in toluene) was spin-coated onto the gold surfaces at 4000 rpm, 1 min. The trimethylsilyl groups were cleaved away and cellulose was generated over hydrochloric vapor (10% solution). Measurements were made at the third overtone (15 Hz). A change in f reflects the amount of mass coupled to the surface of the crystal. For thin, evenly distributed, rigid films, an adsorption induced frequency shift (Δf) is related to the mass uptake as described with the Sauerbrey equation[45]

$$\frac{m}{A} = \frac{Cf}{n_r} \tag{3}$$

where m is the mass (ng), A is the area (cm^2), n_r is the overtone number (= 1, 3, . . .), and C is the mass sensitivity constant (17.7 ng/cm^2/Hz). Measurements were made in triplicate. XG and XG-GRGDS were adsorbed at a concentration of 2 mg/mL. After each adsorption followed a desorption step with water before the cell culture medium was introduced. The same culture medium used in cell seeding was used to study protein adsorption. To elucidate whether the modification with XG-GRGDS resulted in an increase in protein adsorption (and particularly of fibronectin, which is a cell adhesion protein bearing an RGD motif) from the cell culture medium, an antibody against fibronectin (Fibronectin antibody (Biotin; ab6584), Abcam) was introduced after the introduction of the cell culture medium. After all adsorptions followed a desorption step with water.

Wide Angle X-ray Scattering (WAXS). Freeze-dried pellets of BC were pressed into pellets with a diameter of 1 cm. X-ray diffraction patterns were recorded on a Siemens D5000 diffractometer. A Cu Kα anode with a wavelength of 1.54 Å was used. The scanning was made through 2θ = 5–30°. The intensity of the crystal diffraction peak of the amorphous diffraction was measured. The relative crystallinity was determined as the ratio between the crystal part and the total part according to Hermans and Weidinger.[46]

Cell Seeding. Endothelial cells (HSVECs) were isolated from healthy parts of human saphenous veins using an enzymatic method.[47] Cells were cultured in M199 (PAA Laboratories GmbH, Linz, Austria) supplemented with 20% fetal bovine serum (FBS; PAA Laboratories GmbH) with 1.7–3.4 g/dL albumin and a total protein content of 3–4.5 g/mL, penicillin–streptomycin (100 U/mL; PAA Laboratories GmbH), 1.2 mM L-glutamine (PAA), bovine brain extract (75 mg/500 mL; prepared in the laboratory), and heparin (13 U/mL; Leo Pharma, Malmö, Sweden) and kept at 37 °C in a humidified incubator with 5% CO_2. Prior to cell seeding, BC was modified overnight with xyloglucan and XG-GRGDS corresponding to 15% of the dry weight of BC. The modified cellulose was washed 2× with PBS before cell seeding.

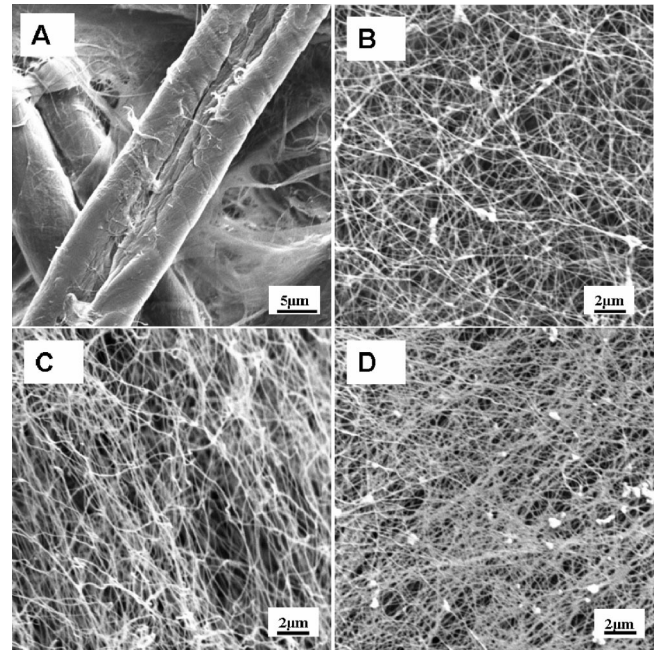

Figure 2. SEM images of cotton linters (A), magnifications at ×2000; BC (B), BC modified with XG-GRGDS (C), and BC after treatment in acetone (D), magnifications at ×5000. Cotton linters have a fibre size of around 6 μm, compared with nanofibrils of 70–100 nm in BC. Untreated BC has the greatest number of pores ≤1 μm. Treatment of BC with XG-GRGDS in an aqueous phase does not affect the morphology. The pore size is the same as that in untreated BC, that is, ≤1 μm. Acetone treatment of BC results in a shrunk network and pores of ≤0.5 μm.

For assessment of cell morphology and adhesion, HSVECs were seeded on pieces of modified and unmodified BC at a density of 3 × 10^5 cells/cm^2. Samples were removed for evaluation at days 1 and 3. Cells were fixed in 3.7% formaldehyde and permeabilized in 0.2% Triton X-100. To visualize f-actin, cells were stained with phalloidin conjugated to Alexa Fluor 546 (Molecular Probes, Inc., Eugene, OR, U.S.A.). The nuclei were counterstained with DAPI (Sigma-Aldrich Sweden AB, Stockholm, Sweden). The specimens were mounted in Slowfade Antifade mounting medium (Molecular Probes, Inc.) and analyzed with a Zeiss LSM 510 Meta (Carl Zeiss, Göttingen, Germany). Pictures were captured digitally. The statistical significance was tested by ANOVA. $P < 0.05$ was considered significant. Field size, $n = 6$.

Results and Discussion

Morphology. The morphology of cotton linters and BC differs in many respects. The cotton linters are composed of fibers whose surface is covered by microfibrils. The size of the fiber is about 6 μm (Figure 2A). BC on the other hand is a swollen three-dimensional network consisting of nanofibrils of a size of 70–100 nm (Figure 2B). Modifying BC with XG in a water phase did not alter the morphology (Figure 2C). This is not the case if modification is done in organic solvents, for example, acetone, where the network clearly shrinks; compare Figure 2B and 2D. To preserve the network of BC, modification in water is preferable. A z-scan in confocal of modified BC with fluorescent XG (XG-FITC) reveals that the nanocellulose material is modified homogeneously throughout (Figure 3).

Specific Surface Area. The specific surface area of the different cellulose substrates was measured using the method of dye adsorption. Yoshida et al. demonstrated that the Langmuir isotherm can be utilized satisfactorily for the adsorption of direct dyes onto cellulose at low dye concentrations.[48] If the adsorbed

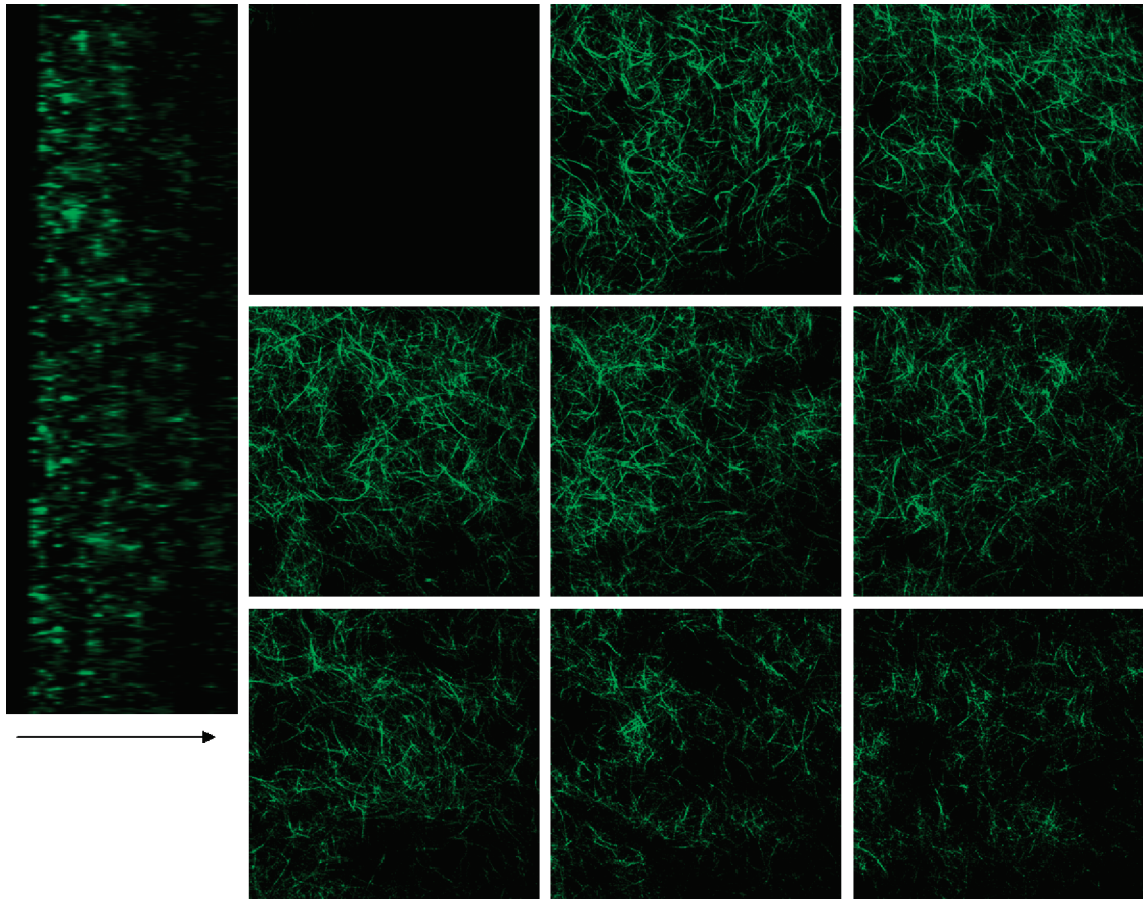

Figure 3. Confocal image of BC modified with XG-FITC. The left image is a cross section of the BC gel, and the arrow indicates the Z-scan direction through the material. The images clearly show that the cellulose is modified throughout the gel.

dye follows the Langmuir isotherm, it has been adsorbed as a monolayer, and the specific surface area can be measured from the maximum adsorption of the dye. The direct dye in this study was Congo Red, and the area occupied by one molecule was calculated by Ougiya et al. to be 1.73 nm^2.[49] The surface area of disintegrated BC with direct dye has been reported by Ouigiya et al. As the present study was conducted on nondisintegrated BC, there was a desire to measure the specific surface area of the gel.

A straight line was obtained from eq 1, suggesting that the adsorption of Congo Red onto both substrates followed the Langmuir model. The Congo Red, thus, most likely adsorbs as a monolayer onto both cellulose surfaces. The adsorption maximum (A_{max}) calculated from the slope value reached 47 mg/g for both surfaces. The specific surface area of BC (79 m^2/g) is more or less the same as that of cotton linters (72 m^2/g) (eq 2). The specific surface area of cotton linters corresponds quite well to values found in the literature for dye adsorption studies,[40,41] while the specific surface of BC was somewhat lower than reported values.[49] This difference was expected, however, as the BC in this case was not disintegrated and most likely had a surface less exposed for adsorption.[43]

XG and XG-GRGDS also followed Langmuir adsorption behavior. The adsorption maximum (A_{max}) of XG and XG-GRGDS reached about 180 mg/g on BC and only about three times as much on cotton linters, see Figure 4B,C. The specific surface area of BC measured with XG and XG-GRGDS was about 200 m^2/g and was almost three times less for cotton linters, 60 m^2/g. Both cellulose surfaces conform to a linear relationship, with larger surface areas corresponding to higher amounts of absorbed XGs.

The difference in the amount of adsorbed XGs can probably be explained by the swollen network of BC and a more exposed and accessible bulk compared to cotton linters. The difference in the specific surface of XG onto the two cellulose substrates might also be due to differences in crystalline structure. BC and cotton linters have the same crystal structure, that is, cellulose I, see Figure 5, and the relative crystallinity is 70% for both substrates. However, the materials have different amounts of the crystalline sub allomorphs (Iα or Iβ), being 60% Iα/40% Iβ in BC and only 30% Iα/70% Iβ in cotton linters. This may influence the physical properties of the cellulose as the allomorphs have different crystal packing, molecular conformation, and hydrogen bonding.

It is known that the size of the adsorbate molecule has a significant influence on the accessible surface area, which leads to the conclusion that less of the cellulose surface is available for adsorption of XGs. The Congo Red molecule is about 2.5 nm in length along its longitudinal axis, while a fully extended XG backbone with DP 26 is around 30 nm.[50] The surface area of cotton linters is higher with Congo Red compared with XG, as expected. The reverse is seen for BC, however, where the surface area measured with XG is larger than that measured with Congo Red. An explanation for this might be the swollen network of BC. The adsorption of polymeric XG to a cellulose surface has been shown to occur with only five XG oligosaccharides. The rest of the XG backbone can form "loops" and "tails" that stick out into the solution.[51] This implies that more XG can be adsorbed on a smaller surface. It is possible that steric effects prevent greater adsorption on cotton linters that are less swollen than BC.

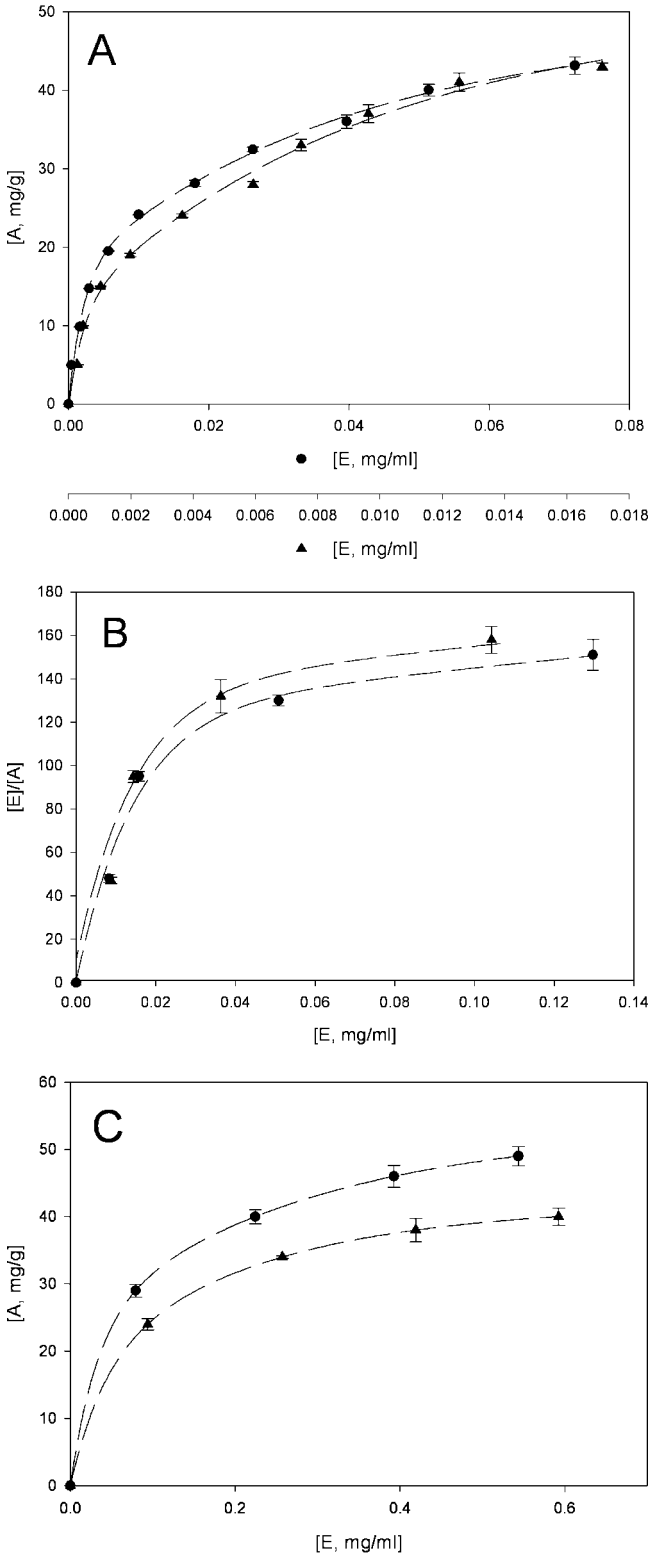

Figure 4. (A) Langmuir adsorption isotherm of BC (▲) and cotton linters (•) dyed with Direct Red 28 (Congo Red), (B) BC adsorbed with XG (•) and XG-GRGDS (▲), and (C) cotton linters adsorbed with XG (•) and XG-GRGDS (▲). Both substrates reach an adsorption maximum, A_{max}, of 47 mg/g Congo Red to the cellulose surface. The A_{max} for XG on BC was slightly lower, 170 mg/g, than XG-GRGDS, 190 mg/g. The A_{max} for XG-GRGDS on cotton linters was slightly lower, 46 mg/g, than for XG itself, whose maximal adsorption is 58 mg/g.

ESCA. ESCA shows that the surface was modified with XGs. A slight increase in the amount of carbons bound to oxygen from the side groups of XGs can be seen. It is impossible to quantify the amount of GRGDS, however, probably as the size of the group is small and might be embedded and pointing toward the interior of the gel when oven-dried. There are also traces of nitrogen in the XG and cellulose themselves, which further complicates the characterization.

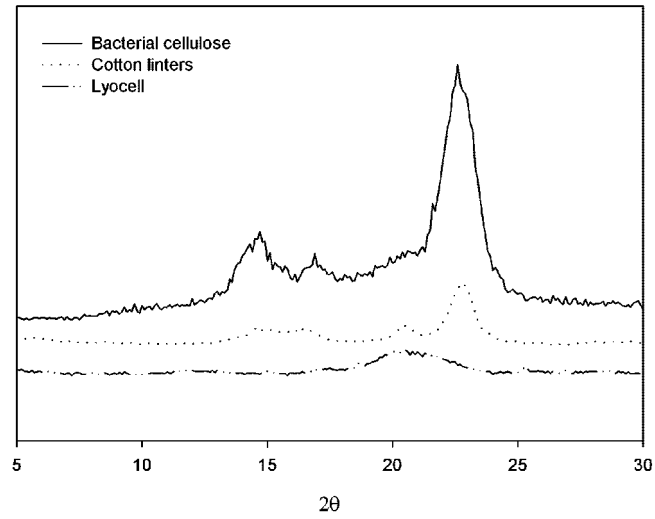

Figure 5. Crystallinity of BC, cotton linters, and lyocell. BC and cotton linters have a relative crystallinity of 70–80% and a crystal structure of cellulose I. Lyocell is regenerated cellulose and has a crystal structure of cellulose II.

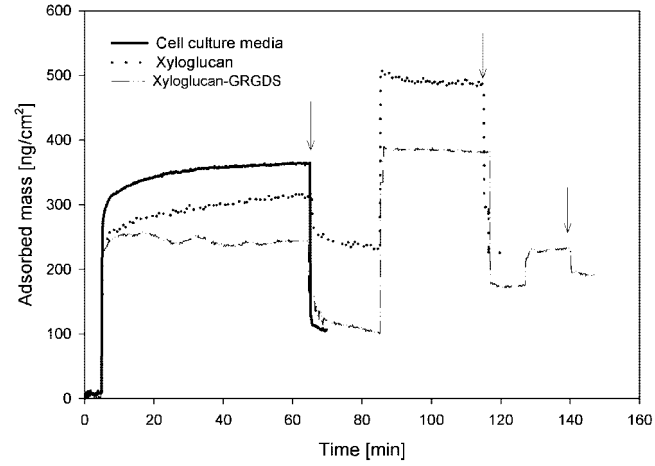

Figure 6. QCM adsorption isotherm of cell culture medium onto cellulose (–), adsorption of XG onto cellulose (···) followed by cell culture medium. XG-GRGDS adsorption onto cellulose (–··) followed by cell culture medium. The arrows represent water wash. Protein (100 ng/cm^2) is adsorbed to the model cellulose surface. XG adsorbs at 230 ng/cm^2 and XG-GRGDS adsorbs at somewhat less, 100 ng/cm^2. XG adsorption did not give an increase in protein adsorption. XG-GRGDS gives less protein adsorption (50 ng/cm^2) than unmodified celluloses. IgG against fibronectin did not adsorb, which indicates that the proteins adsorbed are not the fibronectin adhesion protein.

Contact Angle. The contact angle toward water is somewhat lower when modified with XG (29 ± 4.8) and XG-GRGDS (32 ± 5.8) as compared with that of the unmodified BC (44 ± 5.3). The relatively high contact angle toward water of unmodified BC is due to the compact structure, few pores for capillary forces and few available hydroxyl groups because of the high crystallinity. Modification with XGs increases the number of available hydroxyl groups and, thereby, decreases the contact angle toward water. Introducing a GRGDS did not result in a decrease in wettability; still, the contact angle was lower than that of unmodified cellulose.

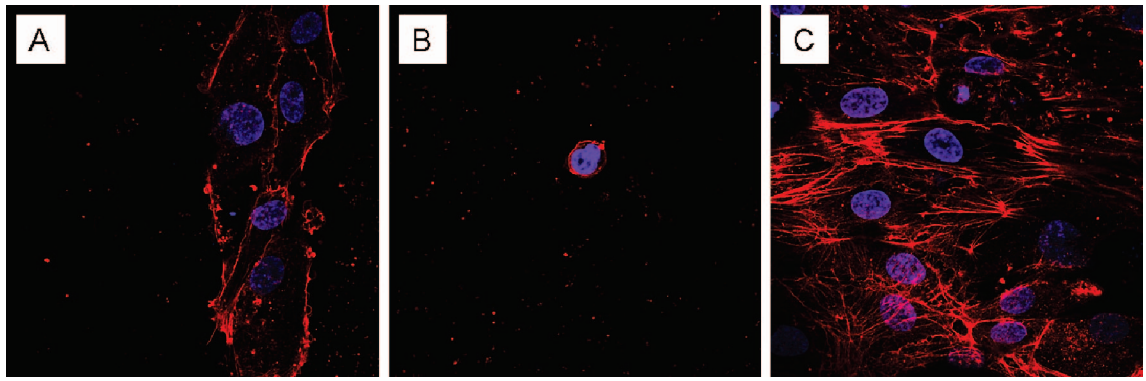

Figure 7. Confocal microscope images of ECs on unmodified BC (A), XG-modified BC (B), and XG-GRGDS-modified BC (C). It is clear that the cell adhesion and spreading of ECs increases when BC is modified with an adhesion peptide.

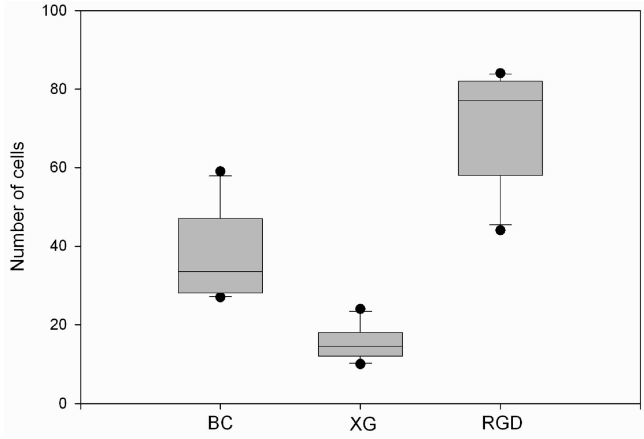

Figure 8. Box plot ($n = 6$) of the number of cells on unmodified BC (BC), XG-modified BC (XG), and RGD-modified BC (RGD). The line dividing the box is the median value being 34 for BC, 15 for XG, and 77 for RGD. The adhesions of cells are significantly higher on RGD-modified BC compared to unmodified and XG-modified BC.

Protein Adsorption. The aim of the modification was to improve human endothelial cell adhesion by introducing a cell specific peptide at the surface. After modification, the material was placed in cell culture medium during cell seeding. The cell culture medium contains a mixture of proteins, including the cell adhesion protein fibronectin bearing a RGD motif. To elucidate whether the modification with XG-GRGDS resulted in an increase in protein adsorption (and particularly in fibronectin) from the cell culture medium, adsorption studies were done on model cellulose surfaces using QCM-D. Around 100 ng/cm^2 of proteins from the cell culture medium was adsorbed to an unmodified cellulose surface (Figure 6). When XG was first adsorbed, no proteins were adsorbed. When the cellulose was modified with XG bearing the adhesion pentapeptide, less protein was adsorbed (50 ng/cm^2) as compared to unmodified cellulose. Antibody IgG against fibronectin was introduced after modification with XG-GRGDS and cell culture medium. IgG against fibronectin did not adsorb, which indicates that the proteins adsorbed are not the fibronectin adhesion protein, or at least not in an activated form. This would thus in later studies of cell proliferation and adhesion tell us that any possible enhancement of endothelial cell adhesion is due to the presence of the RGD epitope on XG and not to a nonspecific adsorption of fibronectin from the cell culture medium. The decrease in contact angle after modification with XG-GRGDS, as mentioned above, might also be correlated to the decrease in protein adsorption after modification.

Cell Adhesion. Initial cell adhesion studies showed that the adhesion of cells occurred more rapidly and was better on the XG-GRGDS-modified cellulose than on the unmodified and XG-modified celluloses. Confocal microscopy images show that there is a greater number of cells on the modified surface and that the extension and adhesion are more developed, see Figure 7. Quantitative data is shown in Figure 8, where the box plot illustrates the data set from six different samples. The median value of cells on BC modified with RGD was 77, on unmodified BC the value was 34, and the value was only 15 when BC is modified with XG. The adhesions of cells are significantly higher on RGD when compared to unmodified and XG-modified BC.

Conclusion

This paper describes a new method to modify cellulose nanofibrils with unaffected morphology of the nanofibril network. BC was successfully modified with XG-GRGDS, as verified using colorimetric methods. The amount adsorbed reached a maximum of 190 mg/g. The nanocellulose material is modified homogeneously throughout the material, as seen by SEM and z-scan in confocal microscopy. Moreover, the modification in the water phase in comparison with organic solvents was clearly advantageous for preserving the morphology. The modification increased the wettability, which might explain the decrease or negligible amount of adsorbed protein shown by QCM-D. Initial cell studies have proven that the adhesion of endothelial cells is improved when the BC hydrogel is modified with XG-GRGDS. The increased cell adhesion was not due to nonspecific adsorption of fibronectin from the culture medium, as demonstrated by QCM-D, but instead to the specific presentation of the RGD epitope by XG. Optimization and proliferation studies of endothelial cells onto BC modified with XG-GRGDS are currently being done at the Vascular Engineering Center, Sahlgrenska University Hospital, Gothenburg.

Acknowledgment. This work was funded by VINNOVA, the Swedish agency for innovation systems, and the Knut and Alice Wallenberg Foundation, who are gratefully acknowledged. We thank Anders Mårtensson for carrying out the SEM analysis and Anne Wendel for the ESCA analysis. We further acknowledge the kind courtesy of Dr. Qi Zhou, KTH Biotechnology, for providing us the XG-FITC and Prof. Allan Esker, Virginia Tech, for the TMSC. Finally, we also thank Dr. Amelie Eriksson-Karlström and Torun Engfeldt (KTH Biotechnology) for assistance with solid phase peptide synthesis. H.B. is a Fellow of the Swedish Research Council (VR Rådsforskare).

References and Notes

(1) Salacinski, H. J.; Goldner, S.; Giudiceandrea, A.; Hamilton, G.; Seifalian, A. M.; Edwards, A.; Carson, R. J. *J. Biomater. Appl.* **2001**, *15*, 241–278.
(2) Mazzucotelli, J. P.; Roudiere, J. L.; Bernex, F.; Bertrand, P.; Leandri, J.; Loisance, D. *Artif. Organs* **1993**, *17*, 787–790.
(3) Gott, V. L.; Whiffen, J. D.; Dutton, R. C. *Science* **1963**, *142*, 1297–1298.
(4) Kobayashi, H.; Kabuto, M.; Ide, H.; Hosotani, K.; Kubota, T. *J. Neurosurg.* **1992**, *77*, 397–402.
(5) Ott, M. J.; Ballermann, B. J. *Surgery* **1995**, *117*, 334–339.
(6) Salacinski, H. J.; Tiwari, A.; Hamilton, G.; Seifalian, A. M. *Med. Biol. Eng. Comput.* **2001**, *39*, 609–618.
(7) Niklason, L. E.; Langer, R. S. *Transplant Immunol.* **1997**, *5*, 303–306.
(8) Kamide, K.; Iijima, H. *Cell. Polym.* **1994**, 189–206.
(9) Miyamoto, T.; Takahashi, S.; Ito, H.; Inagaki, H.; Noishiki, Y. *J. Biomed. Mater. Res.* **1989**, *23*, 125–133.
(10) Suzuki, Y.; Makino, Y. *J. Controlled Release* **1999**, *62*, 101–107.
(11) Diamantoglou, M.; Platz, J.; Vienken, J. *Artif. Organs* **1999**, *23*, 15–22.
(12) Daimon, S.; Saga, T.; Nakayama, M.; Nomura, Y.; Chikaki, H.; Dan, K.; Koni, I.; *Department of Internal Medicine*, Maizuru Kyosai Hospital: Maizuru, Japan, England, United Kingdom, 2000; pp 235–238.
(13) Backdahl, H.; Helenius, G.; Bodin, A.; Nannmark, U.; Johansson Bengt, R.; Risberg, B.; Gatenholm, P. *Biomaterials* **2006**, *27*, 2141–2149.
(14) Helenius, G.; Backdahl, H.; Bodin, A.; Nannmark, U.; Gatenholm, P.; Risberg, B. *J. Biomed. Mater. Res. Part A* **2006**, *76*, 431–438.
(15) Klemm, D.; Schumann, D.; Udhardt, U.; Marsch, S. *Prog. Polym. Sci.* **2001**, *26*, 1561–1603.
(16) Prokop, A.; Wang, T. G. *Ann. N.Y. Acad. Sci.* **1997**, *831*, 223–231.
(17) Peppas, N. A.; Huang, Y.; Torres-Lugo, M.; Ward, J. H.; Zhang, J. *Annu. Rev. Biomed. Eng.* **2000**, *2*, 9–29.
(18) Andrade, J. D., Ed. In *Surface and Interfacial Aspects of Biomedical Polymers*; Wiley & Sons: New York, 1985; *Vol. 1: Surface Chemistry and Physics*.
(19) Riesenfeld, J.; Olsson, P.; Sanchez, J.; Mollnes, T. E. *Med. Device Technol.* **1995**, *6*, 24–31.
(20) Bos, G. W.; Scharenborg, N. M.; Poot, A. A.; Engbers, G. H. M.; Beugeling, T.; Van Aken, W. G.; Feijen, J. *J. Biomed. Mater. Res.* **1999**, *47*, 279–291.
(21) Jeon, S. I.; Lee, J. H.; Andrade, J. D.; De Gennes, P. G. *J. Colloid Interface Sci.* **1991**, *142*, 149–158.
(22) Nagaoka, S.; Mori, Y.; Takiuchi, H.; Yokota, K.; Tanzawa, H.; Nishiumi, S. *Polymer Preprints*; American Chemical Society, Division of Polymer Chemistry: Washington, D.C., 1983; *24*, 67–68.
(23) Merrill, E. W.; Salzman, E. W. *ASAIO J.* **1983**, *6*, 60–64.
(24) Jeon, S. I.; Andrade, J. D. *J. Colloid Interface Sci.* **1991**, *142*, 159–166.
(25) van Wachem, P. B.; Vreriks, C. M.; Beugeling, T.; Feijen, J.; Bantjes, A.; Detmers, J. P.; van Aken, W. G. *J. Biomed. Mater. Res.* **1987**, *21*, 701–718.
(26) Hubbell, J. A.; Massia, S. P.; Desai, N. P.; Drumheller, P. D. *Biotechnology* **1991**, *9*, 568–572.
(27) Massia, S. P.; Hubbell, J. A. *Anal. Biochem.* **1990**, *187*, 292–301.
(28) Massia, S. P.; Hubbell, J. A. *J. Biomed. Mater. Res.* **1991**, *25*, 223–242.
(29) Brumer, H.; Zhou, Q.; Baumann, M. J.; Carlsson, K.; Teeri, T. T. *J. Am. Chem. Soc.* **2004**, *126*, 5715–5721.
(30) Zhou, Q.; Baumann, M. J.; Brumer, H.; Teeri, T. T. *Carbohydr. Polym.* **2006**, *63*, 449–458.
(31) Zhou, Q.; Baumann, M. J.; Piispanen, P. S.; Teeri, T. T.; Brumer, H. *Biocatal. Biotransform.* **2006**, *24*, 107–120.
(32) Kontturi, E.; Thuene, P. C.; Niemantsverdriet, J. W. *Langmuir* **2003**, *19*, 5735–5741.
(33) Matsuoka, M.; Tsuchida, T.; Matsushita, K.; Adachi, O.; Yoshinaga, F. *Biosci. Biotechnol. Biochem.* **1996**, *60*, 575–579.
(34) Greffe, L.; Bessueille, L.; Bulone, V.; Brumer, H. *Glycobiology* **2005**, *15*, 437–445.
(35) Likhosherstov, L. M.; Novikova, O. S.; Derevitskaya, V. A.; Kochetkov, N. K. *Carbohydr. Res.* **1986**, *146*, C1–C5.
(36) Xia, Y.-Q.; Risley, J. M. *J. Carbohydr. Chem.* **2001**, *20*, 45–55.
(37) Eneyskaya, E. V.; Ivanen, D. R.; Shabalin, K. A.; Kulminskaya, A. A.; Backinowsky, L. V.; Brumer, H.; Neustroev, K. N. *Org. Biomol. Chem.* **2005**, *3*, 146–151.
(38) Engfeldt, T.; Renberg, B.; Brumer, H.; Nygren, P. A.; Karlström, A. E. *ChemBioChem* **2005**, *6*, 1043–1050.
(39) Kallas, Å. M.; Piens, K.; Denman, S. E.; Henriksson, H.; Fäldt, J.; Johansson, P.; Brumer, H.; Teeri, T. T. *Biochem. J.* **2005**, *390*, 105–113.
(40) Inglesby, M. K.; Zeronian, S. H. *Cellulose (Dordrecht, Netherlands)* **2002**, *9*, 19–29.
(41) Inglesby, M. K.; Zeronian, S. H. *Cellulose (London)* **1996**, *3*, 165–181.
(42) Kooiman, P. *Recl. Trav. Chim. Pays-Bas Belg.* **1960**, *79*, 675–678.
(43) Ougiya, H.; Watanabe, K.; Matsumura, T.; Yoshinaga, F. *Biosci., Biotechnol., Biochem.* **1998**, *62*, 1714–1719.
(44) Ratner, B. D. *Ann. Biomed. Eng.* **1983**, *11*, 313–336.
(45) Sauerbrey, G. *Z. Phys.* **1959**, *155*, 206–222.
(46) Hermans, P. H.; Weidinger, A. *J. Appl. Phys.* **1948**, *19*, 491–506.
(47) Heydarkhan-Hagvall, S.; Helenius, G.; Johansson, B. R.; Li, J. Y.; Mattsson, E.; Risberg, B. *J. Cell. Biochem.* **2003**, *89*, 1250–1259.
(48) Yoshida, H.; Kataoka, T.; Maekawa, M.; Nango, M. *Chem. Eng. J.* **1989**, *41*, B1–B9.
(49) Ougiya, H.; Hioki, N.; Watanabe, K.; Morinaga, Y.; Yoshinaga, F.; Samejima, M. *Biosci., Biotechnol., Biochem.* **1998**, *62*, 1880–1884.
(50) Hanus, J.; Mazeau, K. *Biopolymers* **2006**, *82*, 59–73.
(51) Vincken, J. P.; de Keizer, A.; Beldman, G.; Voragen, A. G. *Plant Physiol.* **1995**, *108*, 1579–1585.

BM070343Q